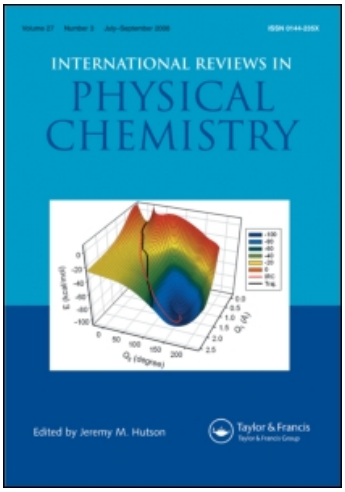

International Reviews in Physical Chemistry
Publication details, including instructions for authors and subscription information:
http://www.informaworld.com/smpp/title~content=t713724383

Gateway-type intramolecular collisional transfer in $^{15}NO(a^4\pi, b^4\Sigma^- \rightarrow B^2\pi)$

J. Heldt[ab]; Ch. Ottinger[a]; A. F. Vilesov[ac]; T. Winkler[a]; D. D. Xu[d]
[a] Max-Planck-Institut für Strömungsforschung, Göttingen, Germany [b] University of Gdansk, Gdansk, Poland [c] Institute of Physics, St. Petersburg State University, St. Petersburg, Russia [d] Dalian Institute of Chemical Physics, Chinese Academy of Sciences, Dalian, People's Republic of China

To cite this Article Heldt, J. , Ottinger, Ch. , Vilesov, A. F. , Winkler, T. and Xu, D. D.(1996) 'Gateway-type intramolecular collisional transfer in $^{15}NO(a^4\pi, b^4\Sigma^- \rightarrow B^2\pi)$', International Reviews in Physical Chemistry, 15: 1, 65 — 76
To link to this Article: DOI: 10.1080/01442359609353175
URL: http://dx.doi.org/10.1080/01442359609353175

INTERNATIONAL REVIEWS IN PHYSICAL CHEMISTRY, 1996, VOL. 15, NO. 1, 65–76

Gateway-type intramolecular collisional transfer in ^{15}NO ($a\,^4\Pi$, $b\,^4\Sigma^- \rightarrow B\,^2\Pi$)

by J. HELDT[1], CH. OTTINGER, A. F. VILESOV[2] and T. WINKLER
Max-Planck-Institut für Strömungsforschung, Bunsenstr. 10, D-37073 Göttingen, Germany

and D. D. XU
Dalian Institute of Chemical Physics, Chinese Academy of Sciences, PO Box 110, Dalian, People's Republic of China

Excitation of ^{15}NO molecules into the $B\,^2\Pi$ state by collisional intramolecular energy transfer from the metastable $a\,^4\Pi$ state was studied under single-collision conditions. Passing a beam of ^{15}NO ($a\,^4\Pi$) through a cell filled with argon at a few mTorr, $B\,^2\Pi \rightarrow X\,^2\Pi$ emission was observed. It originated from only three specific B state levels, namely $^2\Pi_{1/2}$, $J = 21{\cdot}5$ and $^2\Pi_{3/2}$, $J = 21{\cdot}5$ in $v = 2$ and $^2\Pi_{1/2}$, $J = 10{\cdot}5$ in $v = 3$. This selectivity is characteristic of a gateway-type process mediated by spectroscopic perturbations. The analysis showed that in the last case there is a direct spin–orbit interaction of the emitting B state level with a well-specified level of NO(a). The other two perturbations are caused by interactions of the respective NO(B) levels with uniquely identifiable levels of the short-lived NO($b\,^4\Sigma^-$) state, which in turn are collisionally populated from a broad range of NO($a\,^4\Pi$) levels. This latter mechanism is thus a novel type of gateway process. The results explain the anomalous spectral distribution observed in an earlier isotopic study of the $^{15}N^{16}O$ afterglow, which showed an enhanced population of the vibrational levels B, $v = 2$ and 3 [14].

1. Introduction

In spectroscopic studies of the NO molecule the $B\,^2\Pi$ state has special importance, because the optical transition between it and the $X\,^2\Pi$ ground state is allowed ([1–3] and references therein). NO(B) also has a role in the upper atmosphere, since in this region the photodissociation of NO occurs partly via the levels $B\,^2\Pi$, $v \geqslant 7$ excited by sunlight [4]. Figure 1 shows the electronic states of NO relevant to this work. Collisional processes involving the $B\,^2\Pi$ state have also frequently been discussed, largely in connection with the NO afterglow. The band system of particular interest for this work is the β system NO($B\,^2\Pi \rightarrow X\,^2\Pi$), which can be observed in emission from afterglows. Here NO(B) is formed by three-body N + O atom recombination. The mechanism of producing NO(B) under these conditions has been a matter of great interest for a long time ([5–14] and references therein), since the potential energy curve of this state does not connect adiabatically with the energy level of the separate N(^{4}S) and O(^{3}P) atoms (see figure 1).

The following multistep mechanisms have been proposed in order to explain the β band emission [5, 7, 10, 14]. Initially NO($a\,^4\Pi$) is formed by three-body association.

$$N(^4S) + O(^3P) \xrightarrow{M} NO(a\,^4\Pi). \qquad (1)$$

[1] On leave from University of Gdansk, 80-952 Gdansk, Poland.
[2] On leave from Institute of Physics, St. Petersburg State University, St. Petersburg 198904, Russia.

0144-235X/96 $12·00

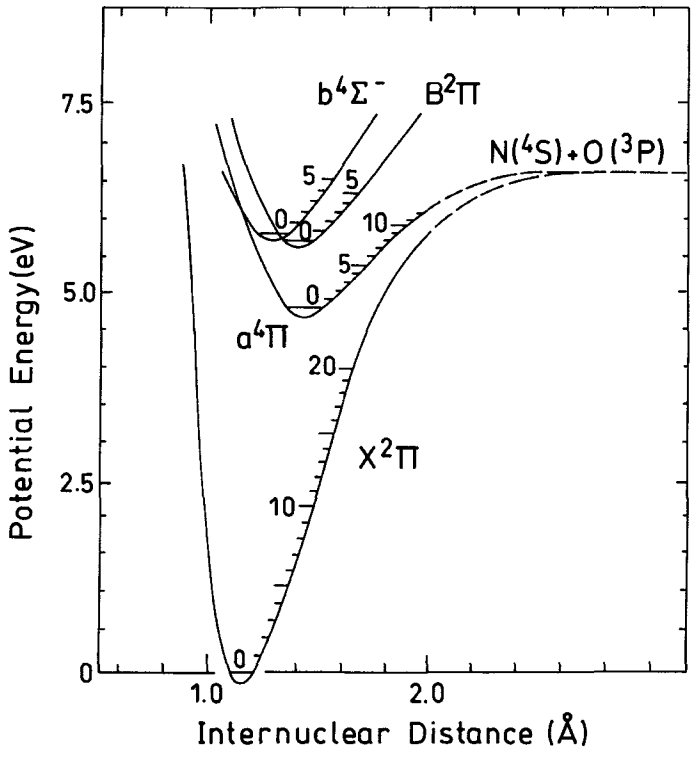

Figure 1. Potential curves of the low-lying states of NO.

This is then followed by intramolecular collision-induced transfer into the radiating **B** state, either directly

$$\mathrm{NO}(\mathbf{a}\,^4\Pi) \xrightarrow{\mathrm{M}} \mathrm{NO}(\mathbf{B}\,^2\Pi), \tag{2}$$

or indirectly via the NO(**b**) state

$$\mathrm{NO}(\mathbf{a}\,^4\Pi) \xrightarrow{\mathrm{M}} \mathrm{NO}(\mathbf{b}\,^4\Sigma^-) \tag{3a}$$

$$NO(\mathbf{b}\,^4\Sigma^-) \xrightarrow{\mathrm{M}} \mathrm{NO}(\mathbf{B}\,^2\Pi). \tag{3b}$$

The reaction sequence (1, 2) has been used to explain certain anomalies in the vibrational distribution of the ^{14}NO(**B**) product. Three types of experiment have all shown that the **B**, $v = 0$ and 3 levels exhibit different characteristics from **B**, $v = 1$ and 2: (a) in ^{14}N + ^{16}O recombination afterglows, the β bands emitted from the $v = 0$ and 3 levels were conspicuously more intense than those from $v = 1$ and 2 [11, 14]; (b) a magnetic field applied on the afterglow reduces the intensities in the former group, but not in the latter [12, 13]; and (c) quenching is more rapid for $v = 0$ and 3 than for $v = 1$ and 2 [10, 15]. The unifying explanation for the special behaviour of the **B**, $v = 0$ and 3 levels has been that they are in close resonance with the **a**, $v = 8$ and 12 levels, spin–orbit coupling providing the link between the two states.

We have recently clarified this assumption in detail, by performing a molecular beam experiment, i.e. employing single-collision conditions [16, 17]. With M being a

light rare gas atom, the NO(**a** → **B**) transition was found to occur almost exclusively (> 95%) through certain specific pairs of rotational/fine structure levels in the **a** and **B** states which are mutually perturbed by spin–orbit (S/O) coupling in the isolated NO molecule. These so-called gateway levels [18–21] facilitate collision-induced transitions in ^{14}NO from the **a**, $v = 8$ and 12 states to the **B**, $v = 0$ and 3 states, respectively [16, 17]. In each case the transition leads to population of only a single specific perturbed rotational/fine structure level, namely $^2\Pi_{3/2}$ (10·5) in **B**, $v = 0$ and $^2\Pi_{1/2}$ (17·5) in **B**, $v = 3$. Our beam experiments on ^{14}NO [16, 17] have thus fully explained the results from the earlier three groups of bulk experiments, where, of course, the kinetic behaviour of specific rotational levels was not observable. The role of the **a** state as a precursor for β band afterglow emission, according to reactions (1, 2), is thus firmly established. The rigorous gateway condition can, however, be relaxed in the case of collisions with heavy atoms or with paramagnetic species. With M = Xe, O_2 or NO, the molecular beam experiments indicated a significant fraction of the collision-induced NO(**a** → **B**) transfer bypassing the specific gateway levels, but still preferring the quasi-resonant vibrational level pairs **a**, 8/**B**, 0 and **a**, 12/**B**, 3. In this case the spin-forbidden **a** → **B** collisional transfer is mediated during the collision by the spin of the collision partner or, in the case of Xe, by the large mass of the collider. The propensity for the near-resonant vibrational levels is then a result of favourable crossings of the potential energy surfaces of the triatomic (NO(**a**) + M)–(NO(**B**) + M) collision system, in contrast to the gateway mechanism, where the extreme selectivity results from a property of the diatomic NO species alone.

In the afterglow studies the reactions (1–3) were also investigated with isotopically substituted N and O atoms [14]. Isotopic substitution caused remarkable changes in the vibrational intensity distribution of the emission from the NO($\mathbf{B}\,^2\Pi$) state. For example, for $^{15}N^{16}O$ strong emission from **B**, $v = 2$ and 3 was observed, while the **B**, $v = 0$ emission was hardly observable at all. This effect was explained by an isotopic shift of the vibrational levels of the **B** state relative to those of the $\mathbf{a}\,^4\Pi$ state, which leads to new vibronic resonances, compared to $^{14}N^{16}O$. The present work was designed to verify this point by extending the molecular beam experiments of [16, 17] to $^{15}N^{16}O$. As expected, β band emission was now observed originating from **B**, $v = 2$ and 3. Thus the findings of the afterglow results are again borne out for this isotopic species. As for ^{14}NO [16, 17], the unrelaxed spectra taken under single-collision conditions reveal the exact pathways of the collisional process. The analysis again shows a highly selective population of specific rotational/fine structure levels, both in **B**, $v = 2$ and 3. However, only with **B**, $v = 3$ does the reaction proceed by a gateway-type energy transfer NO(**a** → **B**) as in ^{14}NO. In the case of the **B**, $v = 2$ emission, there is no near-degeneracy between the emitting **B** state levels and any corresponding level of the **a** state. To explain the selective population of **B**, $v = 2$, the reaction mechanism (1, 3) has to be considered, where step (3*b*) is again of the gateway type. Close energy resonances between the emitting rotational/fine structure levels of **B**, $v = 2$ and corresponding levels of **b**, $v = 1$ could in fact be found, confirming the proposed mechanism (1, 3).

It has been shown [17] that the condition of close energy resonance between the mutually perturbed rotational/fine structure levels **B**, $v = 3$–**a**, $v = 12$ of ^{14}NO yields new spectroscopic information on vibrationally excited levels of NO($\mathbf{a}\,^4\Pi$) as high as $v = 12$. Matching the observed emitting **B**, $v = 3$ level with its perturbing **a** state partner, the latter could be pinpointed with high accuracy. Previously the **a** state levels in this region could only be obtained by extrapolation [13] from the measured data for **a**, $v \leqslant 8$ [22], in combination with much less accurate electron scattering data for $v =$

2–17 [23]. As a result of the experiments of [17], the **a**, $v = 12$ level position was readjusted by $-4{\cdot}4\ \mathrm{cm}^{-1}$. The measurements of the present work, providing a new, independent set of data extending up to the **a**, $v = 12$ level of ^{15}NO, confirm this energy correction. Direct laser excitation of ^{14}NO(**a**) has very recently shown that the **a**, $v = 11$ level is also lower than previously calculated, by an amount of $2{\cdot}6\ \mathrm{cm}^{-1}$ [24]. This is in line with our correction of the $v = 12$ level.

2. Experimental

The experimental arrangement used in this work has been previously described in detail [25, 26]. A collimated supersonic beam of excited ^{15}NO molecules was generated by means of a dc discharge in the beam expansion region. The operating conditions were essentially the same as those used previously [16, 17]. Passing the NO beam through a collision cell filled with Ar and placed at a distance of 25 cm from the discharge, collision-induced optical emission from the cell was observed. The pressure of the target gas in the cell was controlled by two needle valves and was measured by a Baratron model 127 pressure gauge. 1 bar·litre of ^{15}N^{16}O (specified atomic purity 95%) was supplied by IC Chemikalien GmbH, Ismaning. Because of the small quantity of the isotopic gas available and the relatively high gas throughput of the nozzle source, the total duration of the experiment was limited to about 25 minutes.

Light originating from the beam was observed through a quartz window sealed on top of the collision cell. It was collected by a quartz fibre bundle and spectrally resolved by a 0·25 m spectrograph with a 2400 lines/mm grating (1 nm/mm dispersion). The spectra were recorded by a liquid nitrogen-cooled CCD camera. Details of this detector were given in [27]. In this work we used a spectrograph slit width of 100 μm (spectral resolution of 0·15 nm FWHM), with exposure times of 6×100 s (i.e. six consecutive, cumulative exposures of 100 s each, with software-controlled removal of spurious cosmic ray signals in between). Fine wavelength calibration was done by recording Hg lines immediately after the exposure of the ^{15}NO spectrum and superimposed on it, without changing the grating position. We estimate the uncertainty in the measured ^{15}NO line positions to be 0·025 nm. Finally, for comparison, ^{14}N^{16}O collision-induced spectra were also recorded with the same grating setting.

3. Results and discussion

Because of the necessarily very short duration of the experiment, no overview spectrum of the entire emission range 190–440 nm was measured, such as was done [16] for ^{14}NO. It proved to be sufficient to record only relatively narrow sections of the spectrum, where intense bands from the levels of interest were expected: for **B**, $v = 0$, 301·5–315 nm (covered by a single exposure width on the CCD chip of 12 mm length), and for **B**, $v = 1$–4, 240–263 nm (here two adjacent exposure widths were necessary). The most intense ^{15}NO β bands were chosen on the basis of the Einstein coefficients of ^{14}NO from [28], since the Franck–Condon factors depend only slightly on the isotopic species. The results of the measurements are shown in figures 2 and 3. In order to identify the observed emission lines, the line positions of the ^{15}NO β bands were calculated using molecular constants of ^{14}NO [2], rescaled to ^{15}NO in the usual way [29]. The Λ doubling, calculated according to the prescription given in [3], was isotopically scaled following [30].

From figure 2 it can be seen that emission from ^{15}NO is unobservable in the 301·5–315 nm region, in contrast to ^{14}NO, whose reference spectrum is also shown in figure 2. The two small peaks near 305 nm in the lower trace of figure 2 result from a

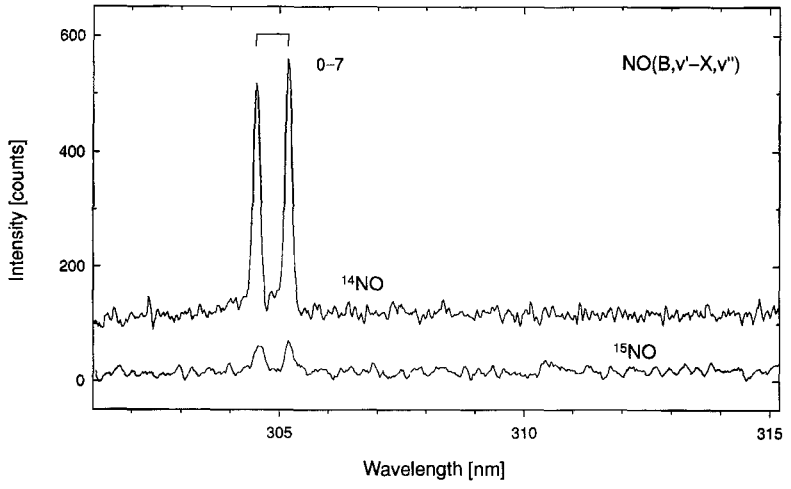

Figure 2. Spectra from a beam of metastable NO molecules colliding with Ar atoms. Target gas pressure 6 mTorr, spectral resolution 0·15 nm FWHM, exposure time 6 × 100 s per section. The spectra are not corrected for the relative sensitivity of the detection system. Lower trace: $^{15}N^{16}O$, showing no detectable emission in this range. Upper trace: $^{14}N^{16}O$, emitting a single P, R line pair from the **B**, $v = 0$ level as identified in [16, 17].

^{14}NO impurity of the sample, which can be estimated from the relative intensities of the lower and upper spectra to amount to about 10 %. The ^{15}NO **B**, 0–**X**, 7 band, which has a good Franck–Condon factor, would be expected to extend across the left half of the region covered by figure 2 (the origin is at 302·1 nm, lines from $J \sim 35$ would lie near 308 nm). From the fact that this band does not appear we conclude that in ^{15}NO the **B**, $v = 0$ level is not populated by reactions (1–3). Strong collision-induced ^{15}NO emission features were, however, observed in the wavelength range 240–263 nm (see figure 3). The analysis shows that they belong to transitions originating from **B**, $v =$ 2 and 3. As with the spectrum of ^{14}NO [16, 17], it can be seen that the emission in these bands is actually concentrated within single rotational/fine structure lines. Table 1 gives the line identifications for these bands. Only the $^2\Pi_{1/2}$, $J = 10{\cdot}5$ level in **B**, $v = 3$ (level I) and the $^2\Pi_{1/2}$, $J = 21{\cdot}5$ and $^2\Pi_{3/2}$, $J = 21{\cdot}5$ levels in **B**, $v = 2$ (levels II and III) are populated. Thus the collisional energy transfer in ^{15}NO is again highly selective, as it was found to be in ^{14}NO. The populated levels are, however, quite different, $v = 3$ and 2 in ^{15}NO versus $v = 3$ and 0 in ^{14}NO. In the two $v = 3$ vibrational levels, different rotational states are populated, $J = 10{\cdot}5$ in ^{15}NO versus $J = 17{\cdot}5$ in ^{14}NO. Comparing the intensities in this latter case one finds them similar (within ~ 30 %) for the two isotopes (compare figure 3 with the ^{14}NO (3, 4) and (3, 5) bands shown in figure 2 of [16]).

As in the case of ^{14}NO [16, 17], the observed selectivity in the population of the **B**, $v = 2$ and 3 states in a collision-induced process arises from a perturbation by an accidental near-degeneracy between a few isolated levels of some precursor state with **B** state levels. For the $^{14}N^{16}O$ isotope such perturbations exist with the **a** $^4\Pi$ state, namely at **B**, $v = 0$, $^2\Pi_{3/2}$ (10·5) with **a**, $v = 8$, $^4\Pi_{5/2}$ (10·5) and at **B**, $v = 3$, $^2\Pi_{1/2}$ (17·5) with **a**, $v = 12$, $^4\Pi_{5/2}$ (17·5) [16, 17]. The comparable intensities of the collision-induced emission for the two isotopes indicate that the efficiency of the perturbation in the present case is about the same, especially for $v = 3$. For $v = 2$ it is less, but here the mechanism is different (see below).

Table 1. Measured and calculated line positions of the ^{15}NO β bands.

Band	Line	λ_{vac} measured (nm)	λ_{vac} calculated (nm)	Emitting level[a]
3–4	$R_1(9{\cdot}5)$	242·634	242·610	I
	$P_1(11{\cdot}5)$	243·037	243·011	
3–5	$R_1(9{\cdot}5)$	253·229	253·260	I
	$P_1(11{\cdot}5)$	253·682	253·693	
2–4	$R_1(20{\cdot}5)$	249·435	249·449	II
	$P_1(22{\cdot}5)$	250·234	250·299	
	$R_2(20{\cdot}5)$	249·985	249·946	III
	$P_2(22{\cdot}5)$	250·821	250·819	
2–5	$R_1(20{\cdot}5)$	260·679	260·684	II
	$P_1(22{\cdot}5)$	261·570	261·603	
	$R_2(20{\cdot}5)$	261·191	261·222	III
	$P_2(22{\cdot}5)$	262·138	262·166	

[a] Emitting levels:
I: $\mathbf{B}\,^2\Pi_{1/2}$, $v = 3$, $J = 10{\cdot}5$, (*e*) and/or (*f*)
II: $\mathbf{B}\,^2\Pi_{1/2}$, $v = 2$, $J = 21{\cdot}5$, (*f*)
III: $\mathbf{B}\,^2\Pi_{3/2}$, $v = 2$, $J = 21{\cdot}5$, (*e*).

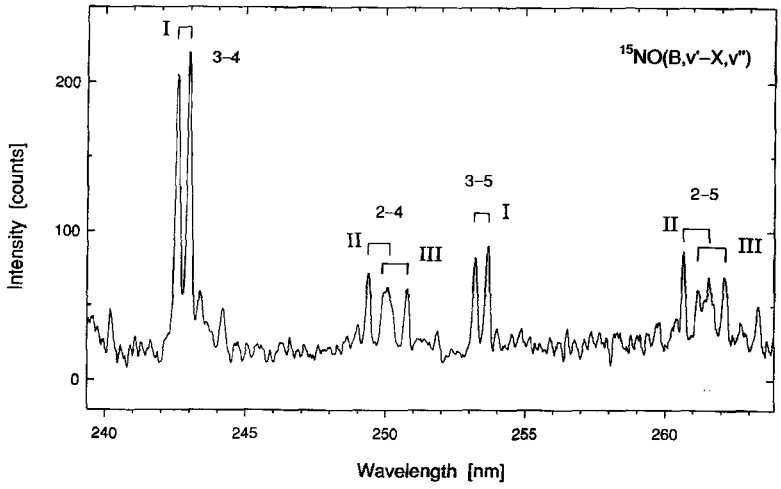

Figure 3. Same as figure 2, at shorter wavelengths, for ^{15}NO. The molecule emits from three very specific **B** state levels. Two series of P, R doublets (marked II and III) belong to the $(2, v'')$ progression, and one (marked I) to the $(3, v'')$ progression. The $v'' = 4$ and 5 members of each progression are shown.

Figure 4 shows the vibrational levels of the electronic states of NO relevant for this work for both isotopic species studied. As the relative positions of the vibrational levels of the **B** and **a** states are shifted by the isotopic substitution, the entire perturbation pattern is also changed. Consequently the spin–orbit coupled levels in **B**, 0 and **a**, 8 of ^{14}NO are shifted off-resonance in ^{15}NO, and the **B**, 0 emission vanishes (figure 2). In order to search for **a** state levels which could be responsible for the perturbation of the three specific $^{15}NO(\mathbf{B})$ levels given above, the rotational/fine structure energies of the $\mathbf{a}, v$ and $\mathbf{B}, v$ levels were calculated on the basis of the best available spectral information for the ^{14}NO molecule [2, 3, 13, 17, 22]. Details can be found in §IV B of

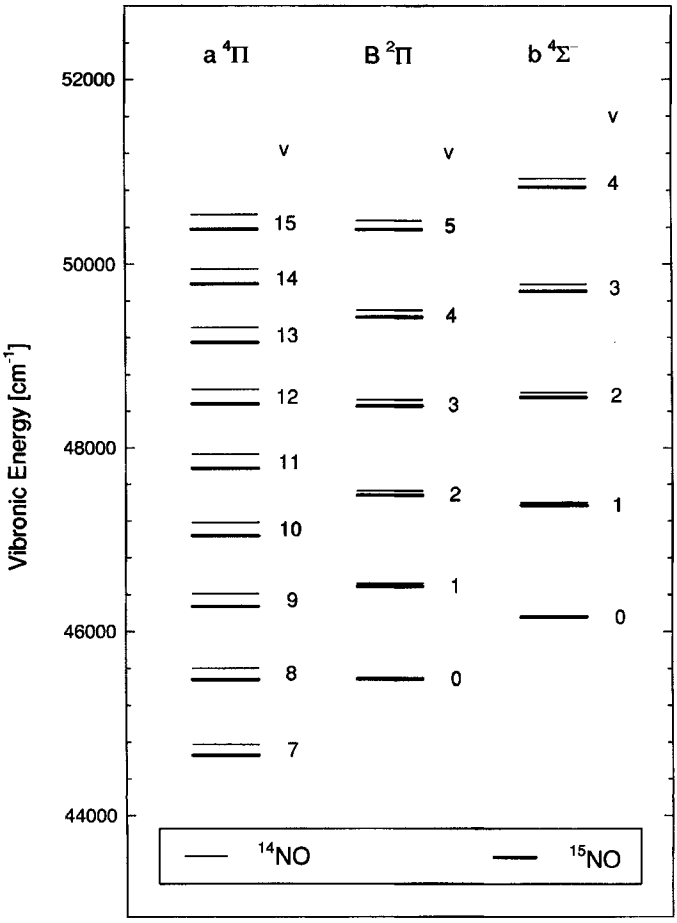

Figure 4. Energies of the rotationless vibrational levels (centre of gravity of the mulitplets) of **a** $^4\Pi$, **B** $^2\Pi$, and **b** $^4\Sigma^-$ for $^{15}N^{16}O$ (thick lines) and, for comparison, for $^{14}N^{16}O$ (thin lines). In the case of $^{14}N^{16}O$ the energies were calculated using the molecular constants for the **X** $^2\Pi$ and **B** $^2\Pi$ states from [2], and for the **a** $^4\Pi$ and **b** $^4\Sigma^-$ states from [22]. Slight corrections for the T_0 value of **a** $^4\Pi$ (and consequently also for T_0 of **b** $^4\Sigma^-$) and for the $v = 12$ level of **a** $^4\Pi$ were included, but are negligible on the scale of this figure. The usual isotopic shift formula was used to calculate the vibrational term energies for the $^{15}N^{16}O$ molecule. Zero energy is at the $v = 0$, $J = 1/2$ level of $^{14}N^{16}O$ ($X\,^2\Pi_{1/2}$). The ^{15}NO **B**, $v = 0$ level lies very slightly *above* the **a**, $v = 8$ level. Since the rotational constant in the **B** state is somewhat larger than in the **a** state, there is then no chance of a close resonance at any higher J between these two states, hence no **B**, $v = 0$ gateway emission is observed in ^{15}NO. For the **B**, 3/**a**, 12 level pair the ordering is the opposite, with **B**, 3 a little below **a**, 12, and in fact **B**, 3 gateway emission does occur in ^{15}NO, at $J = 10{\cdot}5$. For ^{14}NO the separation of this same level pair is greater, and consequently the gateway occurs here at a higher rotational level, $J = 17{\cdot}5$ (see also figure 5).

[17]. In this calculation, the purely vibronic term value of the $v = 0$ level of ^{14}NO(**a** $^4\Pi$) was set at $T_0(\mathbf{a}) = 38266{\cdot}74\ cm^{-1}$, the slightly revised value (decreased by $0{\cdot}46 \pm 0{\cdot}03\ cm^{-1}$) as derived in [17] on the basis of the $^{14}N^{16}O$, **B**, $v = 0$/**a**, $v = 8$ perturbation. More importantly, the much larger correction ($4{\cdot}4\ cm^{-1}$) of the **a**, $v = 12$ level of ^{14}NO from [17] was also used here. The transformation from ^{14}NO to ^{15}NO

Table 2. Characteristics of the identified perturbations between the NO $\mathbf{B}\,^2\Pi$ and $\mathbf{a}\,^4\Pi$, $\mathbf{b}\,^4\Sigma^-$ states for the $^{15}N^{16}O$ isotope.

	Level		Energy (cm^{-1})[a]	$C_{5/2}$	$C_{3/2}$	$C_{1/2}$	$C_{-1/2}$[b]
(I)	$\mathbf{B}, v = 3, {}^2\Pi_{1/2}(10{\cdot}5)$	(*e*)	48581·852		0·29	0·96	
		(*f*)	48581·788				
	$\mathbf{a}, v = 12, {}^4\Pi_{3/2}(10{\cdot}5)$	(*e*)	48581·267	−0·32	0·87	0·38	0·074
		(*f*)	48581·312				
(II)	$\mathbf{B}, v = 2, {}^2\Pi_{1/2}(21{\cdot}5)$	(*f*)	47979·350		0·46	0·89	
	$\mathbf{b}, v = 1, {}^4\Sigma^-_{1/2}(21{\cdot}5)$	(*f*)	47979·445		0·48	0·88	
(III)	$\mathbf{B}, v = 2, {}^2\Pi_{3/2}(21{\cdot}5)$	(*e*)	48035·805		0·89	−0·46	
	$\mathbf{b}, v = 1, {}^4\Sigma^-_{1/2}(21{\cdot}5)$	(*e*)	48035·528		−0·52	0·86	

[a] Calculated from literature data, see text.

[b] Mixing coefficients of the contributing pure Hund's case (*a*) wavefunctions obtained from matrix diagonalization. The matrix elements for **B** were taken from [3], those for **a** and **b** from [22]. The sign convention for the off-diagonal elements follows [3].

was done as described above [29, 30]. Taking into account the requirement of close energy resonance, as well as the selection rules for S/O interaction: $\Delta S = 0, \pm 1, e \leftrightarrow f$, $\Delta J = \Delta\Omega = 0$, the precursor level which is responsible for the observed singular **B**, $v = 3, {}^2\Pi_{1/2}$, $J = 10{\cdot}5$ emission could then be identified to be $\mathbf{a}, v = 12, {}^4\Pi_{3/2}$, $J = 10{\cdot}5$ (fulfilling the $\Delta\Omega = 0$ selection rule by means of rotational Ω-mixing). The fact that this newly-discovered $^{15}N^{16}O$ perturbation at $v = 3$ can thus be explained quite naturally is further confirmation of the revision of the **a** state $v = 12$ vibrational energy.

The matrix element for S/O interaction can be written as

$$V = \sum_{\Omega=1/2,\,3/2} \langle \mathbf{B}, \Omega | H_{SO} | \mathrm{a}, \Omega \rangle \cdot C^{\mathrm{a}}_{\Omega}(J) \cdot C^{\mathrm{B}}_{\Omega}(J) \cdot \langle v_{\mathrm{B}}, J | v_{\mathrm{a}}, J \rangle. \tag{4}$$

The electronic matrix elements were assumed to be the same as for ^{14}NO, which have previously been calculated ([31], table 3, p. 407 and p. 401) to be

$$\langle \mathrm{B}, 1/2 | H_{SO} | \mathrm{a}, 1/2 \rangle = \langle \mathrm{B}, 3/2 | H_{SO} | \mathrm{a}, 3/2 \rangle = -53\ \mathrm{cm}^{-1}. \tag{5}$$

The coefficients $C^{\mathrm{a}}_{\Omega}(J)$ and $C^{\mathrm{B}}_{\Omega}(J)$ were obtained in the course of the matrix diagonalization and are given in table 2. The vibrational overlap integrals $\langle v_{\mathrm{B}}, J | v_{\mathrm{a}}, J \rangle$ were calculated from molecular constants for NO(**B**) [2] and NO(**a**) [22], taking into account the centrifugal potential for the particular rotational state of interest (here $J = 10{\cdot}5$). The value obtained for the S/O interaction matrix element is then $V(\mathbf{B}, 3\text{–}\mathbf{a}, 12) = 8{\cdot}77 \times 10^{-4}\ \mathrm{cm}^{-1}$, of the same order as the previously investigated analogous $V(\mathbf{B}, 3\text{–}\mathbf{a}, 12)$ matrix element in $^{14}N^{16}O$ [17].

For the two ^{15}NO resonances observed in the $\mathbf{B}, v = 2$ level, no near-degeneracy with any **a** state levels could be found. However, close energy resonances (within $<$ $1\ \mathrm{cm}^{-1}$) do exist with the short-lived $\mathbf{b}\,^4\Sigma^-$ state: they are between the *f*-type Λ components at $J = 21{\cdot}5$ *of* $\mathbf{B}, v = 2, {}^2\Pi_{1/2}$ and of $\mathbf{b}, v = 1, {}^4\Sigma^-_{1/2}$, and between the *e*-type Λ components, also at $J = 21{\cdot}5$, of $\mathbf{B}, v = 2, {}^2\Pi_{3/2}$ and of $\mathbf{b}, v = 1, {}^4\Sigma^-_{1/2}$. This suggests another reaction mechanism, according to reactions (1, 3): the long-lived energy carrier is again NO($\mathbf{a}\,^4\Pi$), and in a first step collisional $\mathbf{a} \rightarrow \mathbf{b}$ transfer occurs. This is a facile process, requiring no spin change. It has been studied in some detail for ^{14}NO [16] by means of the resulting $\mathbf{b} \rightarrow \mathbf{a}$ Ogawa band emission, and was found to be of the

non-gateway type, populating a broad range of **b** state rotational levels. Among them are, in the present experiment, those singular **b** levels which are S/O coupled with the two emitting **B**, $v = 2$ levels. The second reaction step, equation (3*b*), is therefore a spontaneous gateway-type process at these particular levels.

Indirect confirmation of this assumed energy flow mechanism is provided by the fact that in ^{14}NO spin–orbit coupling between the **b** and **B** states has actually been observed by Miescher [32]. In the emission spectrum of a discharge ^{14}NO **B**, 1–**b**, 0 and **B**, 2–**b**, 1 perturbations could be detected in certain rotational levels by classical spectroscopic techniques, due to the relatively large S/O coupling matrix elements, $V = 5{\cdot}1$ cm^{-1} and $0{\cdot}4$ cm^{-1}, respectively. These perturbations manifested themselves in considerable shifts of the corresponding **B** state rotational/fine structure levels. It may then appear surprising that these same perturbations did not show up as gateway features in our earlier work on ^{14}NO, by the indirect mechanism (1, 3). One reason may be that the large **B**, 1–**b**, 0 perturbations reported in [32] occur in high rotational levels, mainly in the range $J = 30$–45. Such high levels are hardly populated in the NO(**a**) beam (estimated rotational temperature $\sim$ 150 K, by analogy with an N_2 beam from the same source [25]), but more importantly they are even difficult to access in the collision with the Ar atoms; from data for N_2 collisions given in [33], the mean collision energy is ~ 750 cm^{-1}, corresponding to excitation of levels up to $J \sim 26$. On the other hand, two of the gateways observed in this work do occur at the fairly large $J = 21{\cdot}5$. Therefore an additional factor may have precluded the observation of gateway processes corresponding to Miescher's **B**, 1–**b**, 0 perturbation: the interaction matrix element is here as large as 5 cm^{-1}. According to [34], there is an upper limit for the interaction matrix element V of a well-defined gateway process, given by $V \cdot \tau_{coll} < \hbar$. τ_{coll} is the duration of the collision, in our case $\sim$ 1 ps. This gives $V < 5$ cm^{-1}, and it appears that this condition is violated by the strong **B**, 1–**b**, 0 coupling in ^{14}NO. The failure to observe a gateway process at the ^{14}NO **B**, 2–**b**, 1 perturbation in our earlier work [16, 17] is due to a different reason. Calculating the zero order splitting of the closest matching Λ components of the perturbed **B**, 2–**b**, 1 rotational/fine structure level pairs, one finds very wide gaps of the order of several cm^{-1}. This is considerably greater than the coupling matrix element of $\sim 0{\cdot}4$ cm^{-1}, which may explain why these perturbations were found to be ineffective as gateways in our earlier work [16]. In contrast, the values reported for ^{15}NO in the present work show a very close energy resonance ($0{\cdot}1$ and $0{\cdot}3$ cm^{-1}) of the two **B** state and **b** state level pairs which lead to the observed β line gateway emissions.

The mechanism proposed here for the appearance of the singular **B**, $v = 2$ emission lines is an example of a gateway process where the metastable reservoir state feeds the emitting levels not by collision-induced rotational relaxation within the precursor state itself, but by electronic plus rotational relaxation via a short-lived intermediary. Table 2 summarizes the positions of the perturbed levels of the **B** state as well as the potential perturbers within the **a** and **b** states. This table is similar to table 1 in [17]. A graphic representation of the assigned perturbations in ^{14}NO [16, 17] and ^{15}NO (this work) is shown in figure 5. Note the wide separation of the **b**, $v = 1$ fine structure e and f levels. The selection rule $e \leftrightarrow f$ then makes it possible to clearly identify the perturbed Λ components in **B**, 2, as given in table 2 (e for the $^2\Pi_{3/2}$ perturbation, and f for the $^2\Pi_{1/2}$ perturbation). In the case of the ^{15}NO **B–a** gateway, the present experiments did not allow differentiating between the e and f components. It is possible that both of them are perturbed, as was found to be the case in ^{14}NO [17] on the basis of supplementary LIF experiments.

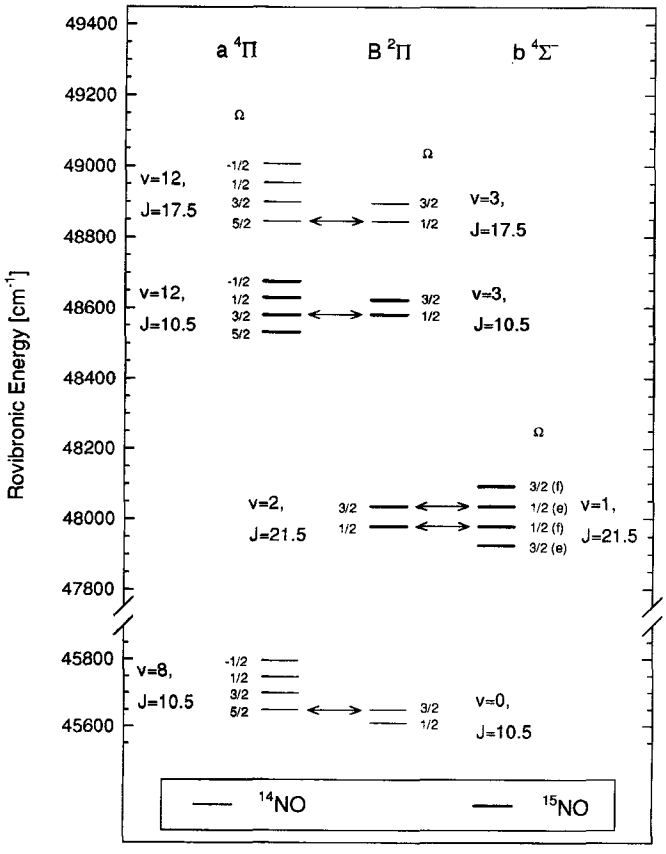

Figure 5. Enlarged section of those regions of figure 4 where perturbations occur: thick lines ^{15}NO; thin lines ^{14}NO. The Λ splitting of the **a** and **B** state levels is too small to be shown. The fine structure splitting of the $\mathbf{b}\,^4\Sigma^-$ level is given in Hund's case (*a*) designation. Perturbed level pairs are indicated by double-headed arrows.

The **b**–**B** S/O interaction matrix elements were calculated in an analogous manner to equation (4): [31], table 3, p. 405 and p. 409 gives the electronic matrix elements as $\sim 10\ cm^{-1}$, and the coefficients $C^b_\Omega(J)$ and $C^B_\Omega(J)$ obtained from the matrix diagonalization are listed in table 2. The calculated S/O interaction matrix elements are then: $V(\mathbf{B}, 2\text{–}\mathbf{b}, 1) = 0{\cdot}630\ cm^{-1}$ for the $J = 21{\cdot}5$ (*f*) case and $-0{\cdot}539\ cm^{-1}$ for the $J = 21{\cdot}5$ (*e*) case.

The gateway mechanism of the NO(**a**, **b**–**B**) energy transfer explains the observed unusual sensitivity of the product state vibrational distribution in the NO afterglow on the isotopic substitution [14]. As with the $\mathbf{B}, v = 0$ and 3 vibrational levels of $^{14}N^{16}O$ [16, 17] the predominant population of the $^{15}N^{16}O$ $\mathbf{B}, v = 3$ level can now also be unambiguously ascribed to a gateway-type energy transfer from the metastable $\mathbf{a}\,^4\Pi$ state. On the other hand, the $\mathbf{B}, v = 2$ level of $^{15}N^{16}O$ is, somewhat unusually, populated via gateways from the short-lived $\mathbf{b}\,^4\Sigma^-$ state. A strong dependence of the chemiluminescence spectrum from the reactions (1–3) on an applied magnetic field, such as was found for ^{14}NO [12], can be predicted to exist also for the isotopically substituted molecules. For example, one can expect the appearance of the $\mathbf{B}, v = 0$ emission from the $^{15}N^{16}O$ isotope upon application of a moderate magnetic field, since

at J values of 1·5–4·5 the calculated zero order **B**, 0 and **a**, 8 rovibronic level energies are separated by less than 2 cm^{-1}.

4. Conclusions

The present work has consolidated the evidence of gateway effects in the energy transfer between doublet and quartet states of NO. Based on previous related observations in ^{14}NO, a strong gateway coupling in ^{15}NO between the $\mathbf{a}\,^4\Pi$ and $\mathbf{B}\,^2\Pi$ states could be identified. In addition, for the first time another, more complex energy transfer path via the $\mathbf{b}\,^4\Sigma^-$ state was shown to exist. This level of detailed insight could only be achieved by taking advantage of the unique properties of molecular beams, which allow single-collision studies of highly excited molecular species.

Acknowledgments

J. Heldt and A. Vilesov thank the Alexander-von-Humboldt-Stiftung for financial support. D. Xu acknowledges gratefully a scholarship from the Max-Planck-Society in cooperation with the Chinese Academy of Sciences.

References

[1] ENGLEMAN, R., JR., ROUSE, P. E., PEEK, H. M., and BAIAMONTE, V. D., 1970, *Beta and Gamma Band Systems of Nitric Oxide*, Los Alamos Scientific Laboratory Report LA-4364.
[2] ENGLEMAN, R., JR., and ROUSE, P. E., 1971, *J. molec. Spectrosc.*, **37,** 240.
[3] FARIS, G. W., and COSBY, P. C., 1992, *J. chem. Phys.*, **97,** 7073.
[4] OKABE, H., 1978, *Photochemistry of Small Molecules* (New York: Wiley).
[5] YOUNG, R. A., and SHARPLESS, R. L., 1963, *J. chem. Phys.*, **39,** 1071.
[6] CAMPBELL, I. M., and THRUSH, B. A., 1967, *Proc. R. Soc. London* A, **296,** 222.
[7] GROSS, R. W. F., and COHEN, N., 1968, *J. chem. Phys.*, **48,** 2582.
[8] CAMPBELL, I. M., and THRUSH, B. A., 1968, *J. Quantum Spectrosc. Radiat. Transfer*, **8,** 1571.
[9] CAMPBELL, I. M., and NEAL, S. B., 1972, *Faraday Discuss. Chem. Soc.*, **53,** 72.
[10] CAMPBELL, I. M., and MASON, R. S., 1976, *J. Photochem.*, **5,** 383; 1978, *ibid.*, **8,** 321; 1978, *ibid.*, **8,** 375.
[11] CAUBET, PH., DEARDEN, S. J., and DORTHE, G., 1984, *Chem. Phys. Lett.*, **108,** 217.
[12] FUKUDA, Y., HAYASHI, H., and NAGAKURA, S., 1985, *Chem. Phys. Lett.*, **119,** 480.
[13] COSBY, P. C., and SLANGER, T. G., 1991, *J. chem. Phys.*, **95,** 2203.
[14] MATVEEV, A. A., PRAVILOV, A. M., and VILESOV, A. F., 1994, *Chem. Phys. Lett.*, **217,** 582.
[15] GADD, G. E., and SLANGER, T. G., 1990, *J. chem. Phys.*, **92,** 2194.
[16] OTTINGER, CH., and VILESOV, A. F., 1994, *J. chem. Phys.*, **100,** 1805.
[17] OTTINGER, CH., and VILESOV, A. F., 1994, *J. chem. Phys.*, **100,** 1815.
[18] GELBARD, W. M., and FREED, K. F., 1973, *Chem. Phys. Lett.*, **18,** 740.
[19] MUKAMEL, S., 1979, *Chem. Phys. Lett.*, **60,** 310.
[20] FREED, K. F., 1981, *Adv. chem. Phys.*, **47,** 291.
[21] TRAMER, A., and NITZAN, A., 1981, *Adv. chem. Phys.*, **47,** 337.
[22] HUBER, K. P., and VERVLOET, M., 1988, *J. molec. Spectrosc.*, **129,** 1.
[23] VICHON, D., HALL, R. I., GRESTEAU, F., and MAZEAU, J., 1978, *J. molec. Spectrosc.*, **69,** 341.
[24] COPELAND, R. A., DYER, M. J., HUESTIS, D. L., and SLANGER, T. G., 1995, *Chem. Phys. Lett.*, **236,** 350.
[25] GEISEN, H., NEUSCHÄFER, D., and OTTINGER, CH., 1987, *Z. Phys.* D, **4,** 263; 1990, *J. chem. Phys.*, **92,** 104.
[26] BACHMANN, R., LI, X., OTTINGER, CH., and VILESOV, A. F., 1992, *J. chem. Phys.*, **96,** 5151.
[27] BACHMANN, R., OTTINGER, CH., and VILESOV, A. F., 1992, *J. chem. Phys.*, **99,** 3262.
[28] PIPER, L. G., TUCKER, T. R., and CUMMINGS, W. P., 1991, *J. chem. Phys.*, **94,** 7667.
[29] HERZBERG, G., 1950, *Molecular Spectra and Molecular Structure, I. Spectra of Diatomic Molecules* (New York: Van Nostrand).

[30] AMIOT, C., BACIS, R., and GUELACHVILI, G., 1978, *Can. J. Phys.*, **56,** 251.
[31] FIELD, R. W., GOTTSCHO, R. A., and MIESCHER, E., 1975, *J. molec. Spectrosc.*, **58,** 394.
[32] MIESCHER, E., 1980, *J. chem. Phys.*, **73,** 3088.
[33] BACHMANN, R., LI, X., OTTINGER, CH., VILESOV, A. F., and WULFMEYER, V., 1993, *J. chem. Phys.*, **98,** 8606.
[34] LEFEBVRE-BRION, H., and FIELD, R. W., 1986, *Perturbations in the Spectra of Diatomic Molecules* (Orlando: Academic Press).